Coastal Engineering Journal

New approach to flap-type wavemaker equation with wave breaking limit

Nino Krvavica, Igor Ružić & Nevenka Ožanić

Published online: 12 Mar 2018.

Submit your article to this journal ⎘

View related articles ⎘

View Crossmark data ⎘

ORIGINAL RESEARCH PAPER

Check for updates

New approach to flap-type wavemaker equation with wave breaking limit

Nino Krvavica ⓘ, Igor Ružić ⓘ and Nevenka Ožanić

Faculty of Civil Engineering, University of Rijeka, Rijeka, Croatia

ABSTRACT
The limitations of the classical wavemaker theory motivated the development of a new equation that can directly predict both regular and broken waves based on the flap-type wavemaker setup. This is achieved first by coupling a commonly accepted wave breaking formula with the linear wavemaker equation. Both these equations were then rewritten in terms of the paddle stroke, water depth, and frequency instead of the wave number. Additionally, the validity range for each equation was explicitly defined to predict the maximum wave height before breaking. Comparison with both classical wavemaker theory and measurements confirms the reliability and accuracy of the proposed equation.

1. Introduction

Studies and tests of water wave interactions with coastal and offshore structures are regularly performed in experimental wave tanks or flumes. Waves are usually generated by an oscillatory motion of a wavemaker. Although many types of wavemakers were developed in the last several decades, the most commonly used are flap (or hinged), piston, and plunger (Dean and Dalrymple 1991).

The relationship between the motion of the wavemaker and resulting waves may be defined by the linear wavemaker theory (Havelock 1929; Biesel and Suquet 1951), which states that the generated wave height H is directly related to the wavemaker stroke S, still water depth d, and wave number $k = 2\pi/L$, where L is the wave length. The wave height to paddle stroke ratio for a flap-type wavemaker is given by the following analytical solution (Dean and Dalrymple 1991):

$$\frac{H}{S} = \frac{4\sinh(kd)}{kd}\frac{kd\sinh(kd) - \cosh(kd) + 1}{\sinh(2kd) + 2kd}, \quad (1)$$

where S is defined as the maximum horizontal distance at the still water level that the paddle travels in one direction from its neutral position (see Figure 3). Equation (1) defines how the wave height to paddle stroke ratio changes for a given depth and wave number.

The first study designed to verify Equation (1) was performed almost 60 years ago by a group of engineers at the Laboratoire Neyrpic (1952). The experiments showed that the measured wave heights were consistently 30% below the values predicted by Equation (1). Ursell, Dean, and Yu (1960) re-evaluated

this theory using a piston type wavemaker and, in contrast, found a very close agreement between the experimental and theoretical results for smaller wave steepness and ~10% lower values than predicted for larger wave steepness. This discrepancy was, at the time, attributed to limitations of the linear wave theory and imperfections in the wavemaker motion (Ursell, Dean, and Yu 1960).

To account for finite amplitude effects, Madsen (1970) extended the linear wavemaker theory to a second-order accuracy. He used a piston-type wavemaker and found a 15% lower wave height than predicted by the nonlinear equation. Therefore, he suggested that these differences should not be attributed to the finite amplitude effects (Madsen 1970). The real reason, he argued, was the leakage around the wavemaker paddle. Madsen (1970) additionally supported his claim by an unpublished technical report by Tenney who demonstrated a significant reduction of wave heights when a hole was drilled in the wavemaker paddle. Furthermore, Fenton (1985) emphasized that in second- or higher-order wavemaker theories, when the wave length is initially unknown, either the wave speed or the mean current of the fluid or the mass flux induced by the waves must be known to accurately obtain the wave length. Otherwise, the extension to a higher-order theory is irrational and is likely to result in the same order of error as in the linear theory (Fenton 1985).

The wavemaker theory was once more thoroughly analyzed and verified by Keating, Webber, and Havelock (1977) using a more sophisticated measuring equipment. They applied a piston-type wavemaker and focused specifically on steeper waves. The results

indicated that the wave heights could be predicted by the linear wavemaker equation to within 6% of error if the leakage around the paddle was minimized. They additionally suggested that a flap-type wavemaker is more suitable for deep water waves, which should additionally reduce the discrepancies. Keating and Webber (1977) also discussed the importance of a reliable prediction of waves generated by a wavemaker. Although knowing the relationship between paddle parameters and wave characteristics is not crucial for regular waves (where generated wave characteristics can be measured directly), it is essential to know this relationship when generating irregular waves by an adaptive control of the wavemaker (Keating, Webber, and Havelock 1977).

In subsequent years, the wavemaker theory was extended for waves with surface tension (Hocking and Mahdmina 1991), for stratified two-layer systems (Mohapatra, Karmakar, and Sahoo 2011), and for porous wavemaker paddles (Chwang 1983; Chakrabarti and Sahoo 1998). Recently, acoustic-gravity waves (AGW) have received much attention in regard to early detection of tsunamis (Stiassnie 2010) or detection of sea-states for wave-power harnessing farms (Tian and Kadri 2017). Therefore, conventional wavemaker theories are currently being adapted for compressible fluids to study the laboratory generation of AGW by wavemakers (Stuhlmeier and Stiassnie 2016; Tian and Kadri 2017).

Today, the wavemaker theory is not only important in planning and executing laboratory experiments, but also in verifying numerical models. More and more frequently, two-dimensional or three-dimensional numerical wave tanks are being developed and applied in studying different wave conditions as an addition or alternative to physical modelling. In the development stage, the numerical wave tanks are being verified by comparing the results to the linear wavemaker theory (e.g. Huang, Zhang, and Lee 1998; Lal and Elangovan 2008; Oliveira, Sanchez-Arcilla, and Gironella 2012; Finnegan and Goggins 2012; Anbarsooz et al. 2013; Saincher and Banerjeea 2015). However, the conventional wavemaker approach has two major limitations for such purposes.

First, the wavemaker theory is valid only for a certain range of wave steepness H/L. In other words, it does not account for wave breaking. If a wavemaker is set to generate a wave that is too steep, the wave would break right on the paddle and the generated wave height would be significantly lower than predicted. For validation purposes, however, it would be more useful if the wavemaker equation could accurately predict both regular and broken wave heights or at least indicate the maximum wave height that can be generated before wave breaking occurs. Although broken waves are rarely used in laboratory experiments, sometimes they are included in the validation of numerical models (e.g. Finnegan and Goggins 2012). Another possible application of broken waves could be in AGW experiments

where much higher frequencies are required in comparison to traditional wave studies (e.g. Stuhlmeier and Stiassnie 2016; Tian and Kadri 2017).

The second difficulty is that Equation (1) is given as a function of the wave number k, whereas the wavemaker is actually controlled by the paddle frequency f (or period $T = 1/f$). These parameters are linked by the implicit wave dispersion relation (Dean and Dalrymple 1991):

$$\omega^2 = gk \tanh(kd), \qquad (2)$$

where $\omega = 2\pi f$ is the angular frequency and g is acceleration of gravity. Therefore, the generated wave height cannot be directly predicted based on the wavemaker setup parameters (paddle stroke, water depth, and frequency). Instead, either the wave length must be measured or the wave number must be found by iteratively solving Equation (2) for a given frequency and depth, before the wave height can be computed by Equation (1). Note that solving Equation (2) is not a problem today; however, explicit expression should be more practical to use. Gilbert, Thompson, and Brewer (1971) recognized this limitation and presented curves for both piston- and flap-type wavemaker as a function of the dimensionless wave period $d/(gT^2)$ rather than the relative water depth kd. Unfortunately, the results were presented only graphically, without any explicit equations.

The aim of this article is twofold and it follows from existing limitations. First, a new wavemaker equation is proposed, which combines both regular and broken waves. This step also includes defining the validity range for each of these equations and the explicit expression for the maximum wave height that can be generated at a given depth. Second, an approximate wavemaker equation is presented in a more practical form – as a function of frequency and depth. In other words, a modified wavemaker equation is derived that answers a theoretical question: what wave height could one expect to be generated when the wavemaker is set to a certain combination of the paddle stroke and frequency at some water depth? More importantly, this study gives an answer to a practical question: what are the maximum wave heights that can be generated before wave breaking occurs? The classical wavemaker theory can only indirectly provide an answer to the first question, and only for a limited range of parameters.

2. Methodology

2.1. Wavemaker equation for regular and broken waves

To define the equation that is valid for both regular and broken waves, Equation (1) should be combined with a corresponding wave breaking equation. A detailed review of wave breaking equations is given

by Rattanapitikon and Shibayama (2000) and Robertson et al. (2013). Because of its inherently variable nature, the understanding of wave breaking process is still an ongoing area of research, but the accuracy of predicting wave breaking parameters has progressed significantly over recent years (Robertson et al. 2013). Many authors have developed different empirical relationships based on small- or large-scale laboratory experiments; most of them are given as a ratio of the broken wave height H_b to the depth at which breaking occurs d_b or to the wave length at the breaking L_b. The resulting equations have many forms and are given as either linear, slope-based, surf similarity parameter, trigonometric, or deep-water wave steepness relationships (Robertson et al. 2013). Since this study is interested in the wave breaking that occurs at the paddle, the trigonometric wave steepness relationship was chosen as the most relevant.

Based on the Stokes wave theory and the assumption that wave breaking occurs when the particle velocity in the wave crest exceeds the wave celerity, Miche (1944) proposed the following equation:

$$H_b = K_b L_b \tanh(k_b d), \qquad (3)$$

where H_b is the broken wave height, L_b is the wave length at breaking, k_b is the wave number for L_b, and K_b is the breaking coefficient. Maximum theoretical wave steepness is defined by $K_b = 0.143$; however, in practical applications, a lower value $K_b = 0.12$ is sometimes recommended (Danel 1952). Battjes and Janssen (1978) modified Equation (3) by introducing an additional parameter γ as follows:

$$H_b = K_b L_b \tanh\left(\frac{\gamma}{0.88} k_b d\right), \qquad (4)$$

where values $\gamma = 0.8$ and $K_b = 0.14$ were proposed based on the calibration with laboratory experiments (Battjes and Janssen 1978). Ostendorf and Madsen (1979) and, recently, Rattanapitikon, Vivattanasirisak, and Shibayama (2003) extended trigonometric wave breaking equations to include bed slope effects.

However, both these formulas may also be used for horizontal beds, in which case they reduce back to Equation (4), with $K_b = 0.14$, $\gamma = 0.704$, and $K_b = 0.14$, $\gamma = 0.8$, respectively.

To combine the wavemaker equation with the wave breaking, Equation (4) is rewritten in terms of the wave height to paddle stroke ratio as follows:

$$\frac{H_b}{S} = K_b \frac{L}{S} \tanh\left(\frac{\gamma}{0.88} k_b d\right). \qquad (5)$$

Furthermore, since paddle stroke depends on depth, it is more appropriate to define the paddle stroke as $S = d \tan\theta$, where θ is the tilting angle of the paddle (see Figure 3). Equation (5) is further modified as follows:

$$\frac{H_b}{S} = K_b \frac{2\pi}{\tan\theta} \frac{\tanh(\gamma k_b d/0.88)}{k_b d}. \qquad (6)$$

Regular and broken waves may, therefore, be predicted by finding a minimum of Equations (1) and (6) for a given wave number, water depth, and paddle angle:

$$\left(\frac{H}{S}\right)_{gen} = \min\left[\frac{H}{S}, \frac{H_b}{S}\right]. \qquad (7)$$

Equation (7) in its dimensionless form (wave height to paddle stroke ratio H/S versus relative depth kd) is illustrated in Figure 1(a) for different paddle angles ranging from 5° to 25°, with $\gamma = 0.8$ and $K_B = 0.14$. This figure shows how a single wavemaker curve (Equation 1) spreads into a set of wave breaking curves (Equation 6) as the relative depth increases. Clearly, the wave height to paddle stroke ratio starts to reduce once the maximum wave steepness is reached. As the wave number increases, wave length becomes shorter, and as a result, the wave height continues to reduce.

Considering that the wavemaker is controlled by the frequency, Equation (7) is also illustrated in Figure 1(b) in a dimensional form. This figure shows one example of the predicted wave heights for a range of frequencies and paddle angles at a 1.0 m depth. In this case, once the breaking limit is reached, all individual wave
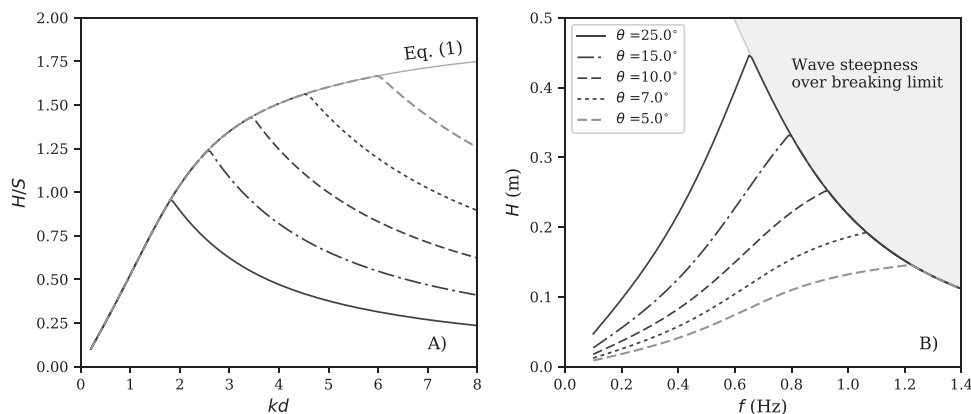
Figure 1. Dimensionless form of a new wavemaker Equation (7) for $\theta = 5–25°$, with $\gamma = 0.8$ and $K_B = 0.14$, (a) H/S versus kd, (b) H versus f for 1.0 m depth.

generator curves (Equation 1) collapse into a single wave breaking curve given by Equation (4).

2.2. Laboratory experiments

To verify the classical wavemaker equation and the newly proposed equation that accounts for broken waves, a series of experiments were carried out in the Hydraulic Laboratory of the Faculty of Civil Engineering at the University of Rijeka. Periodic waves were generated by a flap-type wavemaker in a 12.5 m long experimental flume, with rectangular cross-section, 31 cm wide and 45 cm deep. The flume consists of a stainless steel support and glass reinforced plastic walls. The flap wavemaker consists of a motor with a frequency converter and a crank mechanism that drives the paddle which is fixed to the bottom (Figure 2).

The experimental setup is illustrated in Figure 3. The waves were dissipated by a permeable beach positioned at the other end of the flume. A beach slope of 1:5 was chosen to maximize the dampening, as suggested by Finnegan and Goggins (2012). Some reflection still does occur and, therefore, the wave height slightly varies along the channel. The resulting reflection coefficient ε_r was determined by measurements of wave heights at two locations between the wavemaker and the absorbing beach, as follows (Ursell, Dean, and Yu 1960):

$$\varepsilon_r = \frac{H_r}{H_i} = \frac{H_{max} - H_{min}}{H_{max} + H_{min}} \tag{8}$$

where H_r is the reflected wave height, H_i is the incident wave height, and H_{max} and H_{min} are the respective maximum and minimum values of measured wave heights at the gauges. The first gauge was positioned at a distance of three times the still water depth from the wavemaker, whereas the second gauge was positioned at a distance $\Delta x = 0.4$ m (for $f < 1.0$ Hz) and $\Delta x = 0.15$ m (for $f \geq 1.0$ Hz) from the first gauge. Keating and Webber (1977) showed that a distance of $3d$ from the wavemaker is the optimum positioning of the measuring device, where the evanescent modes produced by the wavemaker completely decay and only the progressive wave is present. The distance of the second gauge was chosen to always fall somewhere in the recommended range $0.05 < \Delta x/L < 0.45$ (Goda and Suzuki 1976).

Water-level oscillations were measured by capacitive gauges and the corresponding wave heights were computed by a *zero-down* crossing method. For all considered combinations of water depths and paddle angles, the reflected wave height was less than 10% of the incident wave heights.

Four sets of measurements were conducted, which combined two different water depths ($d = 19$ and 29 cm) with two different paddle angles ($\theta = 17.3°$ and 25°). Paddle frequencies varied between 0.4 and 2.0 Hz, and the corresponding wave number was determined from the measured wave period by iteratively solving Equation (2). Each experiment run for 5 min to record at least 100 wave periods of the longest waves ($T = 2.5$ s).

3. Results and discussion

3.1. Comparison of measured wave heights with the classical and new wavemaker equation

The generated waves mainly correspond to intermediate water depth ($\pi/10 \leq kd \leq \pi$), but also

Figure 2. Flap-type wavemaker and the experimental flume in the Hydraulic Laboratory of the Faculty of Civil Engineering at the University of Rijeka.
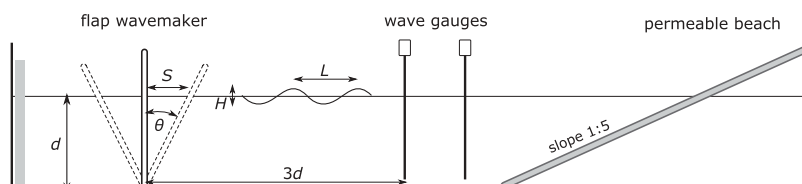

Figure 3. Scheme of the experimental setup (not to scale).

several deep water conditions ($kd > \pi$) were tested. Furthermore, a wide range of waves steepness was considered, so both small steepness ($H/L \leq 0.03$), large steepness ($0.03 < H/L \leq 0.11$), and broken waves ($H/L > 0.11$) were generated. Waves with steepness very close to or over the limit broke right on the paddle; however, they eventually reformed, although the wave profiles were slightly irregular. Keating, Webber, and Havelock (1977) found similar behavior of broken waves in their experiments.

Measured values were first compared to classical wavemaker Equation (1). It seems that in these experiments, both small and large steepness wave heights are slightly below the curve predicted by Equation (1), as shown in Figure 4. However, when the limiting wave steepness is reached, waves break and wave heights decrease as the relative depth increases. Clearly, Equation (1) is not valid for broken waves. For $\theta = 17.3°$, waves break when $kd > 1.7$ with the maximum H/S ratio equal to 0.81, on the other hand, for $\theta = 25°$ waves break when $kd > 2.0$ with the maximum H/S ratio equal to 0.93. These results show that the point at which the wave generator curve losses its validity depends not only on the relative water depth, but also on the paddle angle. This is expected, however, since kd controls the wave length, whereas both kd and θ control the wave height.

For non-broken waves, the wave height to paddle stroke ratio increases with the relative depth as predicted by the classical wavemaker equation. Slightly lower measured values in comparison to Equation (1) could be contributed to the leakage around the paddle, as suggested by Madsen (1970). Leakage is known to cause a loss of wave energy and produce slightly lower wave heights (Keating, Webber, and Havelock 1977).

3.2. Modification of the wavemaker equation by introducing the energy loss coeffcient

To account for the wave height reduction due to leakage, an energy loss coefficient β was introduced, so that Equation (1) is rewritten as follows:

$$\frac{H}{S} = \beta \frac{4 \sinh(kd)}{kd} \frac{kd \sinh(kd) - \cosh(kd) + 1}{\sinh(2kd) + 2kd}. \quad (9)$$

A value $\beta = 0.81$ was found by the regression analysis between the measured and computed values for non-broken waves, with coefficient of determination $R^2 = 0.97$ and a root mean square error (RMSE) 3.3 mm. The discussion on quantifying the loss coefficient due to leakage is left for the next section.

Broken waves, on the other hand, agree well with Equation (6), especially if K_b is calibrated. Again, using regression analysis, a value $K_b = 0.11$ provided the best agreement with the measurements ($R^2 = 0.93$ and RMSE = 4.5 mm). This is lower than $K_b = 0.143$, which is generally used (Miche 1944). However, this higher value is based on a maximum theoretical wave steepness limit, which overestimates broken wave heights in practical applications because some of the energy is dissipated in the breaking process. Battjes and Janssen (1978) used $K_b = 0.14$, whereas Danel (1952) proposed that K_b should be lowered to 0.12 when Equation (4) is applied to horizontal beds. Similarly, Kamphuis (1991) investigated both regular and irregular waves and found that the broken wave height over a horizontal bed could be better predicted when a lower K_b value was used, he proposed 0.095 for irregular and 0.127 for regular waves.

It is reasonable to conclude that the leakage around the paddle could also be responsible for lower K_b values in comparison to other studies. Namely, because of the energy loss due to leakage, the wavemaker is unable to generate a theoretically
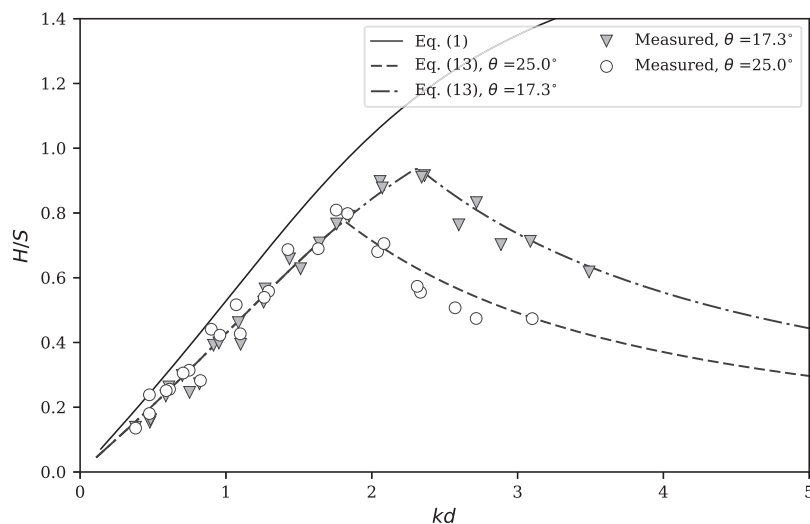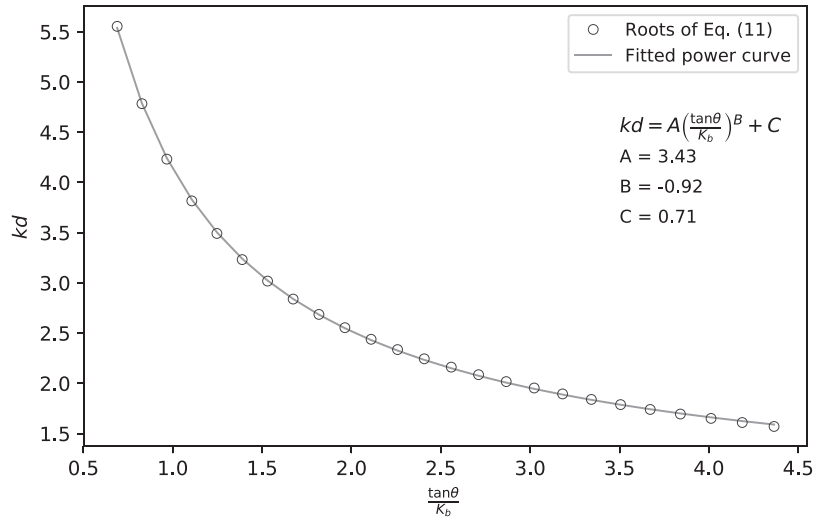

Figure 4. Comparison of measured wave heights with classical Equation (1) and new Equation (13) for $\beta = 0.81$ and $K_b = 0.14$:

Figure 5. Curve fitting of discrete solutions for a maximum relative depth kd given by Equation (11), after which wave breaking occurs.

steepest wave. In fact, $K_b = 0.14$ multiplied by the energy loss coefficient $\beta = 0.81$ results in $K_b = 0.113$, which is almost identical to the calibrated value found in this study. Furthermore, no significant improvement was found with the parameter γ, therefore the wave breaking Equation (6) was redefined to include the energy loss coefficient as follows:

$$\frac{H_b}{S} = \beta K_b \frac{2\pi}{\tan\theta} \frac{\tanh(kd)}{kd}. \qquad (10)$$

The results suggest that when adequate energy loss and breaking coefficients are included, Equation (7) predicts generated wave heights with a high degree of accuracy ($R^2 = 0.97$ and RMSE = 4.1 mm), for both regular and broken waves, and over a wider range of wave numbers, water depths, and paddle angles (see Figure 4).

3.3. Conditional wavemaker equation in terms of wave number and water depth

Although the wave height can be obtained by finding a minimum of two equations (as suggested by Equation 7), it is more convenient to know the relative depth range over which Equation (9) is valid. This range would be limited by the peak relative depth kd_p which corresponds to the maximum wave height before braking for a given depth and paddle angle. The kd_p values are defined by points where Equations (9) and (10) intersect.

These intersection points are found by computing the root of the following equation:

$$\beta \frac{4\sinh(kd)}{kd} \frac{kd\sinh(kd) - \cosh(kd) + 1}{\sinh(2kd) + 2kd}$$
$$= \beta K_b \frac{2\pi}{\tan\theta} \frac{\tanh(kd)}{kd}. \qquad (11)$$

Of course, root of Equation (11) varies with paddle angle θ. Therefore, a set of discrete solutions kd_i that satisfy Equation (11) were individually computed for different

values in the range $\theta_i = 1 - 30°$. Next, a power curve was fitted to a series of points defined by parameters kd_i and $\tan\theta/K_b$, as illustrated in Figure 5. And finally, the following equation for the peak relative depth was obtained (accurate within 1.3% of error):

$$kd_p(\theta) = 3.43\left(\frac{\tan\theta}{K_b}\right)^{-0.92} + 0.71. \qquad (12)$$

The following conditions can, therefore, be defined based on Equation (12):

- for $kd < kd_p$ regular waves are generated as predicted by Equation (9),
- for $kd > kd_p$ broken waves are generated as predicted by Equation (10),
- for $kd = kd_p$ a maximum wave height before breaking is achieved.

Finally, a conditional wavemaker equation is presented for predicting the wave height to stroke ratio for a given wave number and water depth:

$$\frac{H}{S} = \begin{cases} \beta \frac{4\sinh(kd)}{kd} \frac{kd\sinh(kd) - \cosh(kd) + 1}{\sinh(2kd) + 2kd} & \text{for} \quad kd < kd_p \\ \beta K_b \frac{2\pi}{\tan\theta} \frac{\tanh(kd)}{kd} & \text{for} \quad kd \geq kd_p \end{cases}$$
$$(13)$$

where β depends on the amount of leakage around the paddle and K_b is the breaking coefficient. However, Equation (13) should be valid for any flap-type wavemaker, regardless of what value is chosen (or calibrated) for parameters β and K_b. A comparison between measured wave heights and Equation (13) for $\beta = 0.81$ and $K_b = 0.14$ is also shown in Figure 4.

3.4. Conditional wavemaker equation in terms of frequency and water depth

Although for each wave number and depth, a corresponding wave frequency may iteratively be found (as

illustrated in Figure 4), sometimes it is more convenient to have a wave maker equation defined as a function of water depth and frequency. Using trigonometric hyperbolic functions and curve fitting, the following approximation of Equation (9) was found (with 3% of error for $kd < \pi$ and 0.6% of error for $kd \geq \pi$):

$$H \approx 2\beta d \tan\theta \left[1 - \frac{1.03 \tanh\left(0.79\omega^2 d/g\right)^{0.97}}{\left(\omega^2 d/g\right)^{1.02}} \right]. \quad (14)$$

A comparison between the classical wavemaker Equation (9) and the proposed approximate Equation (14) is illustrated in Figure 6(a).

Wave breaking Equation (10) can also be rewritten as a function of the frequency and depth. Since the dispersion equation that defines the relationship between the wave number and wave frequency is implicit, we will base our analysis on its explicit alternative (Guo 2002):

$$kd \approx \frac{\omega^2 d}{g} \left[1 - \exp(-(\omega\sqrt{d/g})^{5/2}) \right]^{-2/5}, \quad (15)$$

which approximates Equation (2) with under 0.75% of error. From Equation (15) it follows that

$$\tanh(kd) \approx \left[1 - \exp(-(\omega\sqrt{d/g})^{5/2}) \right]^{2/5}, \quad (16)$$

therefore, the wave breaking equation can be rewritten as follows:

$$H_b \approx \beta K_b \frac{2\pi g}{\omega^2} \left[1 - \exp(-(\omega\sqrt{d/g})^{5/2}) \right]^{4/5}. \quad (17)$$

A comparison between the proposed approximate Equation (17) and wave breaking Equation (10) is illustrated in Figure 6(b). The comparison is presented for paddle angle θ = 25°, but all other angles show almost identical results.

What remains is to find the peak frequency f_p that defines the validity limit for Equation (14), i.e., defines the maximum wave height before braking. For each relative depth kd_i that satisfies Equation (11), a corresponding dimensionless frequency was found, as follows:

$$\left(\frac{\omega^2 d}{g} \right)_i = kd_i \tanh(kd_i). \quad (18)$$

Next, a power curve was fitted to a series of points defined by parameters $\omega^2 d/g$ and $\tan\theta/K_b$. And, finally, after some algebraic manipulation, the following formula for the peak frequency is obtained (accurate within 2% of error):

$$f_p(d, \theta) = \frac{1}{2\pi} \sqrt{\frac{3.77g}{d} \left(\frac{\tan\theta}{K_b} \right)^{-0.83} + \frac{0.37g}{d}}. \quad (19)$$

Figure 7 shows the curves derived from Equation (19) for different combinations of coefficients and relative paddle angles $\tan\theta/K_b$, which define the validity of the wavemaker theory and delineate the non-breaking from breaking waves.

The following conditions can now be defined based on Equation (19):

- for $f < f_p$ regular waves are generated as predicted by Equation (14),
- for $f > f_p$ broken waves are generated as predicted by Equation (17),
- for $f = f_p$ a maximum wave height before breaking is achieved.

Finally, a new conditional equation is obtained for directly predicting generated wave heights for a given water depth, paddle angle, and frequency.

$$H(f, d, \theta) \approx \begin{cases} 2\beta d \tan\theta \left[1 - \frac{1.03 \tanh\left(3.16\pi^2 f^2 d/g\right)^{0.97}}{\left(4\pi^2 f^2 d/g\right)^{1.02}} \right] & \text{for } f < f_p \\ \beta K_b \frac{g}{2\pi f^2} \left[1 - \exp(-(4\pi^2 f\sqrt{d/g})^{5/2}) \right]^{4/5} & \text{for } f \geq f_p \end{cases}, \quad (20)$$

The comparison of measured values and Equation (20) is illustrated in Figure 8 for each measured depth and paddle angle. Note that the two-step process does not increase the complexity of obtaining the wave height, since the classical approach also requires that the wave dispersion equation is solved before the wave height to paddle stroke ratio can be obtained.
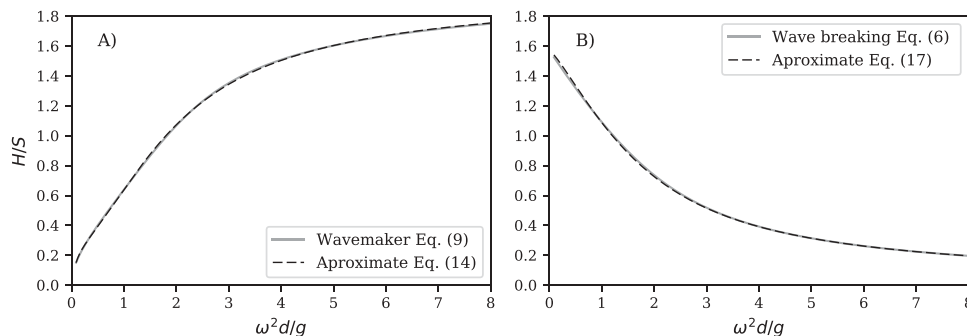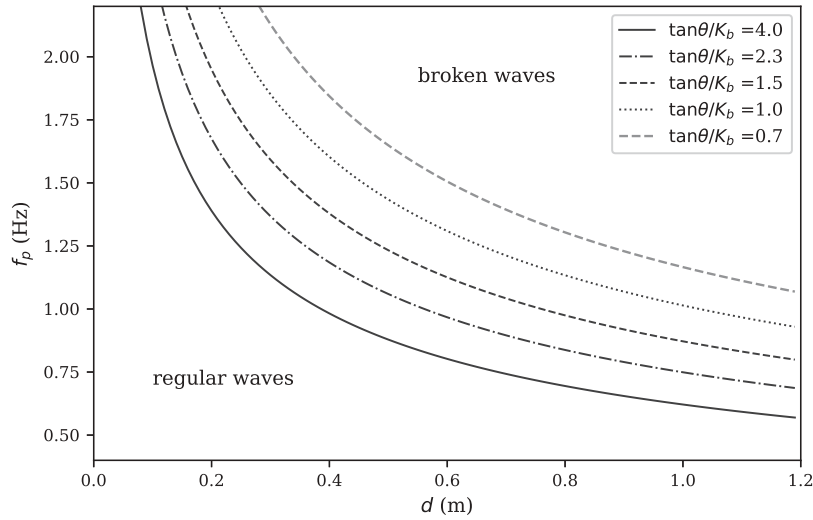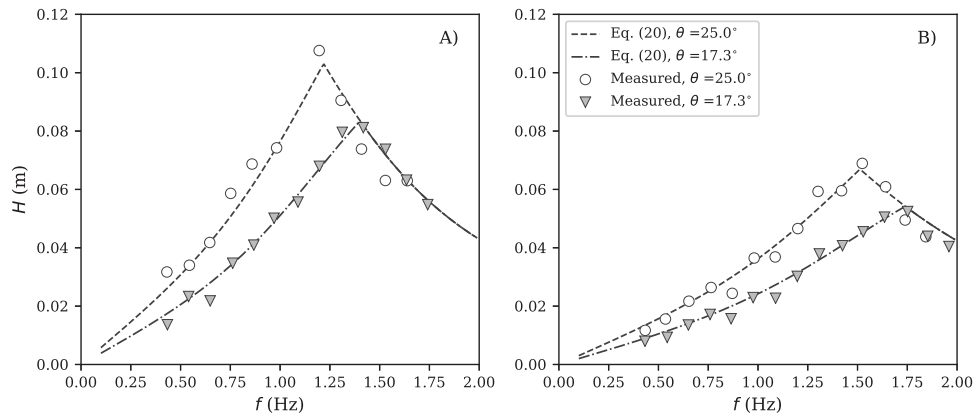

Figure 6. Comparison of: (a) wavemaker Equation (9) to approximate Equation (14) and (b) wave breaking Equation (10) to approximate Equation (17) for $\theta = 25°$.

Figure 7. Set of curves (Equation 19) that define the maximum frequency for a given depth after which wave breaking occurs.


Figure 8. Comparison of the measured wave heights and Equation (20) with $\beta = 0.81$ and $K_b = 0.14$ for different paddle angles at depth: (a) $d = 29$ cm and (b) $d = 19$ cm.

To summarize, Equation (7) is a general way of mathematically describing a new approach that combines the classical wavemaker equation with a wave breaking formula to predict both regular and broken waves generated by a flap-type wavemaker. Equation (13) in comparison to Equation (7) is written as a combined equation with explicitly defined boundaries of validity, which additionally includes the energy loss coefficient β to account for the leakage around the paddle. Equation (20), on the other hand, is an approximation of Equation (13), which should produce almost the same results. The only difference between these two equations is that the former is explicitly defined and therefore the results can be computed directly for a given water depth, paddle angle and frequency. Equations (7), (13), and (20) are shown side-by-side in Figure 9 to illustrate their similarities and differences.

4. Effect of the leakage around the paddle

In this study, the effects of leakage were accounted for by introducing an energy loss coefficient, which was computed by linear regression between the measured and
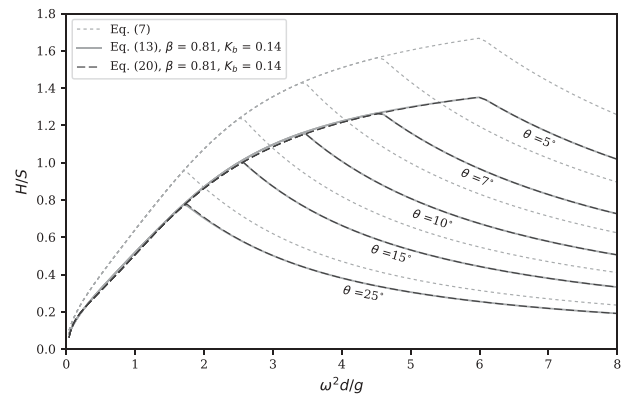
Figure 9. Equations (7), (13), and (20) in terms of relative frequency for $\theta = 5$–25°.

theoretical values for non-broken waves. However, this reduction in wave heights can be predicted based on wave characteristics and the ratio of the gaps to the flume cross section. Madsen (1970) proposed the following analytical expression for the wave height reduction which accounts for the leakage under and through the sides of the paddle (Madsen 1970):

$$\frac{\Delta H}{H} = -\left[2.22\frac{\Delta b}{d}\sqrt{\frac{1}{\cosh kd}}\frac{kd}{\sinh kd}\right.$$
$$\left.+1.11\frac{\Delta s}{b}\left(1+\sqrt{\frac{1}{\cosh kd}}\right)\right]\frac{gH}{2U^2} \qquad (20)$$

where ΔH is the difference between generated and theoretical wave heights, Δb is the size of the gap between the paddle and flume bottom, Δs is the size of the gap between the flume walls and the paddle, b is the flume cross-section width, and U is the wavemaker velocity averaged over depth. Note that the energy loss coefficient is related to the height reduction as $\beta = 1 - \Delta H/H$.

In the current experiments, the paddle is connected to the flume bottom by a rubber strip to eliminate any leakage under the paddle; however, the gap between a 31 cm wide paddle and flume walls is $\Delta s = 14$ mm (4.5%). For current wavemaker setup, Equation (21) predicts wave height reductions ranging from 17% to 39% (with a mean value of 25.1% and standard deviation 5.3%). This is in good agreement with average reduction of 20.7% (standard deviation 8.1%) obtained from comparing measured and theoretical wave heights. A close value was also obtained using linear regression to compare measured and theoretical wave heights, where a constant 19% reduction resulted in the smallest root mean square error (RMSE = 3.3 mm).

A similar difference was found in the Madsen's experiment (1970), where a wave height reduction of 15% was measured for a 3% leakage area. Oliveira, Sanchez-Arcilla, and Gironella (2012) found a $8.2 - 8.9\%$ reduction for $\Delta b = 1.2$ cm, $\Delta s = 1.0$ cm, and $b = 40$ cm. Keating, Webber, and Havelock (1977) showed that when leakage is minimized, height reduction may become lower than 5%. However, Wu et al. (2016) studied generation of solitary waves by a wavemaker and numerically analyzed the influence of leakage around the paddle. They found that the leakage is still apparent even for a very a small gap of just 0.24%. Although Madsen's expression produced reliable prediction of an average wave height reduction in the present study, fully understanding the influence of leakage is, clearly, still an unresolved issue, which requires further experimental and numerical investigation.

5. Conclusion

A combined wavemaker equation for both regular and broken waves was presented in this study. The limitations of the classical wavemaker equation for the prediction of wave heights based on specific paddle angles and frequencies at a certain water depth were demonstrated. The first limitation is that the wavemaker theory is not valid for broken waves. The second, more practical difficulty, is that the wavemaker is sometimes implicit in

predicting the wave height based on the experimental setup (water depth and paddle frequency).

The first problem was solved by combining the linear wavemaker theory with a wave breaking equation, which was expressed as a wave height to paddle stroke ratio. The proposed Equation (13) indicated a close agreement with small-scale laboratory measurements for both regular and broken waves generated by a flap-type wavemaker. Furthermore, a relative depth limit that defines the maximum wave height before breaking was explicitly defined (Equation 12). However, waves that break at the paddle are not sufficiently investigated; therefore additional measurements are needed to instill more confidence in the combined equation.

The second difficulty was resolved by deriving an approximate Equation (20) for both the wavemaker and wave breaking equation expressed in terms of the water depth, paddle angle, and frequency. Comparisons of approximate results against both classical equations and measurements indicated a satisfactory agreement. Furthermore, a frequency limit that denotes the validity range of the wavemaker theory and the maximum wave heights before breaking was also explicitly defined (Equation 19).

To conclude, the proposed equation should be valid and applicable for any flap-type wavemaker, under the assumption that the energy loss and breaking coefficient are determined by the calibration. Also, it should be straightforward to derive a similar approximation for a piston-type wavemaker by following the methodology presented here.

Disclosure statement

No potential conflict of interest was reported by the authors.

Funding

ORCID

Nino Krvavica http://orcid.org/0000-0001-5014-5476
Igor Ružić http://orcid.org/0000-0003-4964-7190

References

Anbarsooz, M., M. Passandideh-Fard, and M. Moghiman. 2013. "Fully Nonlinear Viscous Wave Generation in

Numerical Wave Tanks." *Ocean Engineering* 59: 73–85. doi:10.1016/j.oceaneng.2012.11.011.

Battjes, J. A., and J. Janssen. 1978. "Energy Loss and Set-Up Due to Breaking of Random Waves." *Coast Engineering* 1978: 569–587.

Biesel, F., and F. Suquet. 1951. "Laboratory Wave Generating Apparatus." *La Houille Blanche* 2: 147–165.

Chakrabarti, A., and T. Sahoo. 1998. "The Effect of Surface Tension in Porous Wave Maker Problems." *The Journal of the Australian Mathematical Society. Series B. Applied Mathematics* 39: 539–556. doi:10.1017/S0334270000007797.

Chwang, A. T. 1983. "A Porous-Wavemaker Theory." *Journal Fluid Mechanisms* 132: 395–406. doi:10.1017/S0022112083001676.

Danel, P. 1952. On Limiting Clapotis, Gravity Waves. *National Bureau of Standards, Circular* 521: 35–45. US Department of Commerce.

Dean, R. G., and R. A. Dalrymple. 1991. *Water Wave Mechanics for Engineers and Scientists (Vol. 2)*. Singapore: World scientific publishing Co.

Fenton, J. D. 1985. "A Fifth-Order Stokes Theory for Steady Waves." *Journal of Waterway, Port, Coastal, and Ocean Engineering* 111 (2): 216–234. doi:10.1061/(ASCE)0733-950X(1985)111:2(216).

Finnegan, W., and J. Goggins. 2012. "Numerical Simulation of Linear Water Waves and Wave-Structure Interaction." *Ocean Engineering* 43: 23–31. doi:10.1016/j.oceaneng.2012.01.002.

Gilbert, G., D. Thompson, and A. Brewer. 1971. "Design Curves for Regular and Random Wave Generators." *Journal of Hydraulic Research* 9 (2): 163–196. doi:10.1080/00221687109500345.

Goda, Y., and Y. Suzuki. 1976. "Estimation of Incident and Reflected Waves in Random Wave Experiments." *Coastal Engineering Proceeding* 48 (15): 828–845.

Guo, J. 2002. "Simple and Explicit Solution of Wave Dispersion Equation." *Coastal Engineering* 45 (2): 71–74. doi:10.1016/S0378-3839(02)00039-X.

Havelock, T. H. 1929. "LIX. Forced Surface-Waves on Water." *The London, Edinburgh, and Dublin Philosophical Magazine and Journal of Science* 8 (51): 569–576. doi:10.1080/14786441008564913.

Hocking, L. M., and D. Mahdmina. 1991. "Capillary-Gravity Waves Produced by a Wavemaker." *Journal Fluid Mechanisms* 224: 217–226. doi:10.1017/S0022112091001726.

Huang, C.-J., E.-C. Zhang, and J.-F. Lee. 1998. "Numerical Simulation of Nonlinear Viscous Wavefields Generated by Piston-Type Wavemaker." *Journal of Engineering Mechanics* 124 (10): 1110–1120. doi:10.1061/(ASCE)0733-9399(1998)124:10(1110).

Kamphuis, J. W. 1991. "Incipient Wave Breaking." *Coastal Engineering* 15: 185–203. doi:10.1016/0378-3839(91)90002-X.

Keating, T., N. Webber, and T. H. Havelock. 1977. "The Generation of Periodic Waves in a Laboratory Channel: A Comparison between Theory and Experiment."

Proceedings of the Institution of Civil Engineers 63 (4): 819–832. doi:10.1680/iicep.1977.3078.

Lal, A., and M. Elangovan. 2008. "CFD Simulation and Validation of Flap Type Wave-Maker." *World Academy of Science, Engineering and Technology* 4 (1): 76–82.

Madsen, O. S. 1970. "Waves Generated by a Piston-Type Wavemaker." *Coast Engineering* 1970: 589–607.

Miche, A. 1944. "Mouvements ondulatoires de la mer en profondeur constante ou dcroissante." *Annales des Ponts et Chausses* 25: 369–406.

Mohapatra, S. C., D. Karmakar, and T. Sahoo. 2011. "On Capillary Gravity-Wave Motion in Two-Layer Fluids." *Journal Engineering Mathematical* 71 (3): 253–277. doi:10.1007/s10665-011-9451-y.

Neyrpic. 1952. "Laboratory Wave Generating Apparatus. From the User's Viewpoint." *La Houille Blanche* 6: 779–801.

Oliveira, T. C. A., A. Sanchez-Arcilla, and X. Gironella. 2012. "Simulation of Wave Overtopping of Maritime Structures in a Numerical Wave Flume." *Journal App Mathematical* 2012: 1–19.

Ostendorf, D. W., and O. S. Madsen. 1979 "An Analysis of Longshore Current and Associated Sediment Transport in the Surf Zone." Report No. 241, Department of Civil Engineering. 1165–1178. MIT.

Rattanapitikon, W., and T. Shibayama. 2000. "Verification and Modification of Breaker Height Formulas." *Coastal Engineering Journal* 42 (4): 389–406. doi:10.1142/S0578563400000195.

Rattanapitikon, W., T. Vivattanasirisak, and T. Shibayama. 2003. "A Proposal of New Breaker Height Formula." *Coastal Engineering Journal* 45 (1): 29–48. doi:10.1142/S0578563403000634.

Robertson, B., K. Hall, R. Zytner, and I. Nistor. 2013. "Breaking Waves: Review of Characteristic Relationships." *Coastal Engineering Journal* 55 (1): 1350002–1350040. doi:10.1142/S0578563413500022.

Saincher, S., and J. Banerjeea. 2015. "Design of a Numerical Wave Tank and Wave Flume for Low Steepness Waves in Deep and Intermediate Water." *Procedia Engineering* 116: 221–228. doi:10.1016/j.proeng.2015.08.394.

Stiassnie, M. 2010. "Tsunamis and Acoustic-Gravity Waves from Underwater Earthquakes." *Journal Engineering Mathematical* 67: 23–32. doi:10.1007/s10665-009-9323-x.

Stuhlmeier, R., and M. Stiassnie. 2016. "Adapting Havelock's Wave-Maker Theorem to Acoustic-Gravity Waves." *IMA Journal of Applied Mathematics* 81 (4): 631–646. doi:10.1093/imamat/hxw003.

Tian, M., and U. Kadri. 2017. "Wavemaker Theories for Acousticgravity Waves over a Finite Depth." *Journal Engineering Mathematical*. doi:10.1007/s10665-017-9902-1.

Ursell, F., R. G. Dean, and Y. Yu. 1960. "Forced Small-Amplitude Water Waves: A Comparison of Theory and Experiment." *Journal Fluid Mechanisms* 7 (1): 33–52. doi:10.1017/S0022112060000037.

Wu, N.-J., S.-C. Hsiao, H.-H. Chen, and R.-Y. Yang. 2016. "The Study on Solitary Waves Generated by a Piston-Type Wave Maker." *Ocean Engineering* 117: 114–129. doi:10.1016/j.oceaneng.2016.03.020.